Identification of bacterial lipopeptides as key players in IBS

Camille Petitfils[1]*, Sarah Maurel[1]*, Gaëlle Payros[1], Amandine Hueber[2,3], Bahija Agaiz[1], Geraldine Gazzo[4], Rémi Marrocco[5], Frédéric Auvray[1], Geoffrey Langevin[6], Jean-Paul Motta[1], Pauline Floch[1,7], Marie Tremblay-Franco[8,9], Jean-Marie Galano[6], Alexandre Guy[6], Thierry Durand[6], Simon Lachambre[5], Anaëlle Durbec[2,3], Hind Hussein[10], Lisse Decraecker[10], Justine Bertrand Michel[2,3], Abdelhadi Saoudi[5], Eric Oswald[1,7], Pierrick Poisbeau[4], Gilles Dietrich[1], Chloé Melchior[11], Guy Boeckxstaens[10], Matteo Serino[1], Pauline le Faouder[2,3#], Nicolas Cenac[1#].

[1] IRSD, Université de Toulouse-Paul Sabatier, INSERM, INRAe, ENVT, UPS, Toulouse, France
[2] MetaboHUB-MetaToul, National Infrastructure of Metabolomics and Fluxomics, Toulouse, France
[3] I2MC, Université de Toulouse, Inserm, Université Toulouse III – Paul Sabatier (UPS), Toulouse, France.
[4] Centre National de la Recherche Scientifique, Université de Strasbourg, Institut des Neurosciences Cellulaire et Integrative (INCI), Strasbourg, France.
[5] INFINITY, Université de Toulouse-Paul Sabatier, INSERM, CNRS, UPS, 31000 Toulouse, France
[6] Institut des Biomolécules Max Mousseron (IBMM), UMR 5247, CNRS, Université de Montpellier, ENSCM, Montpellier, France
[7] CHU Toulouse, Hôpital Purpan, Service de bactériologie-hygiène, Toulouse, France
[8] Toxalim (Research Center in Food Toxicology), Toulouse University, INRAE, ENVT, INP-Purpan, UPS, F-31027 Toulouse, France.
[9] Metatoul-AXIOM Platform, MetaboHUB, Toxalim, INRAE, F-31027 Toulouse, France.
[10]Laboratory of Intestinal Neuro-immune Interaction, Translational Research Center for Gastrointestinal Disorders, Department of Chronic Diseases, Metabolism and Ageing, KU Leuven, Leuven, Belgium.
[11]Rouen University Hospital, Gastroenterology Department and INSERM CIC-CRB 1404, and INSERM UMR 1073, Institute for Research and Innovation in Biomedicine, Normandy University, Rouen, France. Current address: Department of Molecular and Clinical Medicine, Institute of Medicine, Sahlgrenska Academy, University of Gothenburg, Gothenburg, Sweden.

* Joint first author
# Joint last author

Index

Supplementary methods

Colorectal distension

Nickel-chrome electrodes were implanted in the abdominal external oblique musculature of anesthetized mice in order to detect EMG activity as previously described [1]. CRD was performed 3 days post-surgery by inserting a distension catheter (Fogarty catheter for arterial embolectomy, 4 F; Edwards Lifesciences, Nijmegen, Netherlands) into the colon at 5 mm from the anus. The balloon was progressively inflated in a stepwise of 15mmHg (from 0 to 60mmHg) performing 10s distension for each pressure and with resting intervals of 5min (n=14-19 mice/group, 3 independent experiments). In a second set of experiments, mice submitted to stress (n=15 per group, 2 independent experiments) were treated with a 100µL intracolonic injection of C14snGABA (10µM) or its vehicle (EtOH 40%) 30min before CRD. The results were expressed as the area under the curve from 15 to 60mmHg.

Permeability and macro and microscopic scores

To determine paracellular permeability, mice were gavaged with dextran 4kDa-FITC (25mM; Sigma, St. Quentin Fallavier, France). Four hours after, mice were sacrificed. Blood was collected for FITC quantification in the serum and colons were removed. Length and thickness were measured and macroscopic colonic tissue damages were scored from 0 to 3 for the intensity of adhesion and strictures, from 0 to 2 for the intensity of edema, erythema, ulceration and diarrhea and from 0 to 1 (absent or present) for the mucus, hemorrhage and fecal blood; the maximal score being 17. For histological examination, a piece of colon located at 2cm proximal to the anus was resected, fixed in 10% phosphate buffered formalin, embedded in paraffin, sectioned, and stained with hematoxylin–eosin. Slides were examined and graded for cellular infiltration, mucosal architecture alteration and submucosal oedema from 0 to 3 (absent, mild, moderate and severe) and vasculitis, muscular thickening, crypt abscess and goblet cell depletion from 0 to 1 (absent or present); the maximal score being 13.

Real time PCR analysis

Colon biopsies were crushed in 500µL of Trizol (Invitrogen, Thermofisher scientific, Saclay, France) in Precellys lysing kit tubes (Bertin Technologies, Montigny le Bretonneux, France) placed in a Precellys (2823g, 30 seconds twice; Bertin Technologies). After addition of

chloroform and centrifugation (15 minutes, 11292 g at 4°C), the supernatant containing the RNA was removed. Ethanol 70% (vol/vol) was added and the contents were placed in columns (GenElute® mammalian total RNA miniprep kit, Sigma Aldrich). The RNA was extracted according to the manufacturer recommendations. Subsequently the RNA was dosed in a nanodrop (implenGmbH, Dominique Dutscher, Issy-les-Moulineaux, France). RNA (3µg) preparations from colon of mice were used for the total RNA reverse-transcription with Moloney murine leukemia virus reverse transcriptase (Fisher Scientific) using random hexamers (Fisher Scientific) for priming. Transcripts encoding Hypoxanthine phosphoribosyl transferase (Hprt), Trefoil factor 3 (Tff3), Mucin 2 (Muc2), Occludin (Ocln), Zonula occludens-1 (Tjp1), Regenerating islet-derived 3 gamma (Reg3γ), Matrilysin (Mmp7), Tumor necrosis factor alpha (Tnfα), Chemokine (C-Cmotif) ligand 5 (Ccl5), Transforming growth factor beta (Tgfβ), Interleukin 6 (Il6), Interleukine 1 beta (Il1β), Nuclear factor kappa B (Nfκb), Chemokine (C-X-C motif) 2 ligand Cxcl2, Lipoxygenase 15 (Alox15), Lipoxygenase 5 (Alox5), Lipoxygenase 12 (Alox12), Cyclooxygenase 1 (Ptgs1), Cyclooxygenase 2 (Ptgs2), Pro-enkephaline (Penk), Interferon gamma (Ifnγ), Peroxysome proliferator-Activated Receptor(PPARα), Acyl-CoA Thioesterase 12 (Acot12), Angiopoietine like 4 (Angptl4), Cluster of differenciation 36 (CD36), Aryl hydrocarbon receptor (Ahr), glucocorticoid receptor (Nr3C1) and soluble epoxy hydrolase (Ephx2), were quantified by real-time PCR using specific forward and reverse primers (**Table S3**), the kit Takyon SYBR 2X MasterMix blue dTTP (Eurogentec) and the LightCycler480II (Roche Diagnostics, Meylan, France). Hierarchical clustering was performed, and heat maps were obtained with R (www.rproject.org). Gene expressions were transformed to z scores and clustered based on 1− Pearson correlation coefficient as distance and the Ward algorithm as agglomeration criterion.

Liquid chromatography/tandem mass spectrometry (LC-MS/MS) measurements

PUFA metabolites were quantified from mice colons by mass spectrometry after lipid extraction as previously described [2]. After the addition of 500µL of PBS, and 5µL deuterated Internal Standard (IS) mixture (5-HETEd8, LxA4d4 and LtB4d4), the colons were crushed in lysing MatrixA tubes in a precellys (Bertin Technologies). After two crush cycles (6.5 ms−1, 30s), 10µL of suspensions were withdrawn for protein quantification and 0.3mL of cold methanol (MeOH) were added. The samples were centrifuged at 1016 × g for 15min (4°C) and the resulting supernatants were submitted to solid phase extraction of lipids using HLB plate

(OASIS® HLB 30 mg, 96-well plate, Waters, Saint-Quentin-en-Yvelines, France). Briefly, plates were conditioned with 500µL MeOH and 500µL H2O/MeOH (90:10, v/v). Samples were loaded at a flow rate of about one drop per 2s and, after complete loading, columns were washed with 500µL H2O/MeOH (90:10, v/v). The phase was thereafter dried under aspiration and lipids were eluted with 750µL MeOH. Solvent was evaporated under N2 and samples were resuspended with 140µL MeOH and transferred into a vial (Macherey-Nagel, Hoerdt, France). Finally, the 140µL of methanol were evaporated and our sample resuspended with 10µL of methanol for liquid chromatography/mass spectrometry analysis. 6-keto-prostaglandin F1 alpha (6kPGF$_{1\alpha}$), thromboxane B2 (TxB2), Prostaglandin E2 (PGE$_2$), 8-iso Prostaglandin A2 (8-isoPGA$_2$), Prostaglandin E3 (PGE$_3$), 15-Deoxy-Δ12,14-prostaglandin J2 (15d-PGJ$_2$), Prostaglandin D2 (PGD$_2$), Lipoxin A4 (LxA4), LxB4, Resolvin D1 (RvD1), Resolvin D2 (RvD2), Resolvin D5 (RvD5), 7-Maresin 1 (7-Mar1), Leukotriene B4 (LtB4), Leukotriene B5 (LtB5), Protectin Dx (PDx), 18-hydroxyeicosapentaenoic (18-HEPE), 5,6-dihydroxyeicosatetraenoic acid (5,6-DiHETE), 9-hydroxyoctadecadienoic acid (9-HODE), 13-hydroxyoctadecadienoic acid (13-HODE), 15-hydroxyeicosatetraenoic acid (15-HETE), 12-hydroxyeicosatetraenoic acid (12-HETE), 8-hydroxyeicosatetraenoic acid (8-HETE), 5-hydroxyeicosatetraenoic acid (5-HETE), 17-hydroxydocosahexaenoic acid (17-HDoHE), 14-hydroxydocosahexaenoic acid (14-HDoHE), 14,15-epoxyeicosatrienoic acid (14,15-EET), 11,12-epoxyeicosatrienoic acid (11,12-EET), 8,9-epoxyeicosatrienoic acid (8,9-EET), 5,6-epoxyeicosatrienoic acid (5,6-EET), 5-oxoeicosatetraenoic acid (5-oxoETE), Prostaglandin F2α, (PGF$_{2\alpha}$), 13-Hydroxyoctadecadienoic acid (13oxoODE), 9-hydroxyoctadecadienoic acid (9oxoODE), 10-hydroxyoctadecadienoic acid (10-HODE), 9,10-dihydroxy-12-octadecenoic acid (9,10-DiHOME), 12,13-dihydroxy-12-octadecenoic acid (12,13-DiHOME), 9-hydroxy-10,12,15-octadecatrienoic acid (9-HOTrE), 13-hydroxy-9,11,15-octadecatrienoic acid (13-HOTrE), 9,10,13-trihydroxy-11-octadecenoic acid (10-TriHOME) and 9,12,13-trihydroxy-11E-octadecenoic acid (12-TriHOME) were quantified in mouse colons. To simultaneously separate 42 lipids of interest and three deuterated internal standards (5-HETEd8, LxA4d4 and LtB4d4), LC-MS/MS analysis was performed on an ultrahigh-performance liquid chromatography system (UHPLC; Agilent LC1290 Infinity) coupled to an Agilent 6460 triple quadrupole MS (Agilent Technologies) equipped with electrospray ionization operating in negative mode. Reverse-phase UHPLC was performed using a Zorbax SB-C18 column (Agilent Technologies) with a gradient elution. The mobile phases consisted of water, acetonitrile (ACN), and formic acid (FA) [75:25:0.1 (v/v/v)] (solution A) and ACN and FA

[100:0.1 (v/v)] (solution B). The linear gradient was as follows: 0% solution B at 0 min, 85% solution B at 8.5min, 100% solution B at 9.5min, 100% solution B at 10.5min, and 0% solution B at 12 min. The flow rate was 0.4ml/min. The autosampler was set at 5°C, and the injection volume was 5µL. Data were acquired in multiple reaction monitoring (MRM) mode with optimized conditions. Peak detection, integration, and quantitative analysis were performed with MassHunter Quantitative analysis software (Agilent Technologies). Blank samples were evaluated, and their injection showed no interference (no peak detected), during the analysis. Hierarchical clustering was performed, and heat maps were obtained with R (www.rproject.org). PGJ2, RVD1, RVD2, RVD5, 7Mar1, 5,6-DiHETE were not detected in our samples. PUFA metabolite amounts were transformed to z scores and clustered based on 1− Pearson correlation coefficient as distance and the Ward algorithm as agglomeration criterion.

Dosage of the corticosterone

Mice were anesthetized with ketamine/xylasine and submandibular blood was collected into tubes and centrifuged (15min, 8000rpm) to separate the serum. Serum samples were stored at -80°C until analysis. Corticosterone levels were determined using the corticosterone AlphaLISA detection kit (PerkinElmer, AL3020C) following manufacturer's instructions. The volumes of all reagents were adjusted for the use 5µl of serum or standard. The serum samples were diluted 1:5 into 1X diluent. The corticosterone concentrations in serum samples were expressed in ng/ml. (n=8 to 10 mice/group).

Phenotypic analysis of mesenteric lymph node cells

11 weeks old controls or prenatally stressed mice were euthanized and their mesenteric lymph node cells were stained with conjugated antibodies for flow cytometry analysis. The monoclonal antibodies (mAbs) used for flow cytometry were as follows: anti-TCRαβ-BV711(H57-597), anti-CD4-BV786, (GK1.5), anti-CD8α-A700 (53-6.7), anti-CD44-Percep5.5 (IM7) and anti-CD62L-APC (MEL-14), and with a viability dye (APC-H7) to exclude dead cells. We used the Foxp3/transcription factor permeabilization kit according to the manufacturer's instructions (e-Biosciences) to fix and permeabilize the cells prior to intracellular staining with anti-Foxp3 labelled antibody (Foxp3-BV421 (FJK-16s)). The fluorescently conjugated antibodies were purchased from e-Biosciences, BD Biosciences, and Biolegend. Data were collected on LSR-Fortessa cytometer (BD Biosciences) and analyzed using the FlowJo software.

Fecal bacterial DNA extraction

Feces were collected and frozen at -80°C until use. 15 feces/ group chosen from 3 independent experiments. Metagenomic DNA was extracted from the feces using a QIAamp DNA Stool Mini Kit (Qiagen, Hilden,Germany) according to the manufacturer's instructions. Quickly, the feces were crushed in the inhibitex buffer at (6.5 ms−1, 3x30 s), placed at 95°C and then were centrifuged 2min, at 16 000g, at room temperature to pellet the stool particles. 200µL of the supernatant were added to 15µL of proteinase K and AL buffer and incubated 10min at 70°C. 200µL of EtOH were added and the samples were added in the spin columns and centrifuged at 16 000g at room temperature for 1 minute. The supernatant was removed and 500µL of washing buffer 1 was added. After centrifugation at 16 000g at room temperature for 1 minute, the supernatant was removed and 500µL of washing buffer 2 was added. After centrifugation at 16 000g at room temperature for 3 minutes, the supernatant was removed and 50µL of the elution buffer was added. Finally, the samples were centrifuged for 1 minute at 16 000g at room temperature and the DNA was collected. The DNA was then quantified using a Nanodrop.

Taxonomic and predicted functional analysis of gut microbiota

Total DNA was extracted from freshly-collected snap-frozen feces as already described [3]. The 16S rRNA gene V3-V4 regions were targeted by the 357wf-785R primers and analyzed by MiSeq at RTLGenomics (http://rtlgenomics.com/, Texas, USA). An average of 29795 sequences was generated per sample. A complete description of the applied bioinformatic filters is available (http://www.rtlgenomics.com/docs/Data_Analysis_Methodology.pdf). LDA scores were drawn by the Huttenhower Galaxy web application (http://huttenhower.sph.harvard.edu/galaxy/) via the LEfSe algorithm [4]. The predictive functional analysis (gut microbiome) of gut microbiota was performed via PICRUSt [5]. Diversity indices were calculated with the software PAST4 [6].

Biofilm

For fluorescent *in situ* hybridization, a specimen of colon with a feces was resected, fixed in carnoy (60% MeOH, 30% chloroform, 10% acetic acid), embedded in paraffin, sectioned, and labelled with the universal bacterial 16 S fluorescent rRNA probe EUB338-Cy3, 5'-GCTGCCTCCCGTAGGAGT-3'Cy5, Eurofins) at 10µL/mL, wheat germ agglutinin-FITC 1/1000

(Sigma-Aldrich L4895) was used to stain the polysaccharide-rich mucus layer, and the epithelial cell nucleus was stained with DAPI (ProLong Gold antifade reagent with DAPI, Invitrogen P36935). Bacterial penetration into the mucus was measured by image processing on Fiji by quantifying the number of 16S RNA labelled pixel between the edge of the lumen to the edge of the epithelium (n=12 mice/group; 4 images/mice, 2 independent experiments). The mucus zone was manually traced, and an arbitrary distance was assigned to each pixel from the middle to the epithelial cells border. Cyanine 5 labelled pixels in this zone were assigned to their corresponding distance. The distance of each pixel in regard to the luminal compartment and the number of labeled pixels between the edge of the lumen to middle of the mucus (Apical) and between the middle of the mucus to the edge of the epithelium (Basal) were quantified.

Identification of colonic mouse bacteria

Ligilactobacillus murinus strain IRSD_2020, *Limosilactobacillus reuteri* and *Lactobacillus johnsonii/gasseri* were isolated from mouse intestinal mucosa on *Lactobacillus* selection agar (BD Diagnostic, Le Pont de Claix, France), and identified by matrix-assisted laser desorption/ionisation time-of-flight mass spectrometry (Microflex LT MALDI-TOF MS, Bruker Daltonik GmbH, Germany). Whole genome sequencing of *Ligilactobacillus murinus* strain IRSD_2020 has been performed as well as the quantification of this strain and of *Ligilactobacillus animalis* by Taqman® real-time PCR. *Ligilactobacillus murinus* strain IRSD_2020 was cultured and GABA-containing lipopeptides quantified.

Whole genome sequencing of *Ligilactobacillus murinus* IRSD_2020

Genomic DNA from *L. murinus* IRSD_2020 and *L. animalis* DSMZ 20602 were purified from 200 µL overnight cultures with MagNA Pure 96 DNA and Viral NA Small Volume Kit (Roche Diagnostics France SAS, Meylan, France) and sequenced in 2x150 bp paired-end by illumina® NextSeq500 (IntegraGen SA, Evry, France) with an 80x coverage. Libraries were obtained by enzymatic fragmentation using a 5X WGS Fragmentation mix kit (Enzymatics Inc., Beverly, MA, USA). The sequence data generated were deposited in the NCBI BioProject database (https://www.ncbi.nlm.nih.gov/bioproject/) under the accession the number PRJNA770189.

Quantification of *Ligilactobacillus murinus* IRSD_2020 and *Ligilactobacillus animalis* using TaqMan® real-time PCR

Primers and probes included in the real-time PCR assay targeting *L. murinus* were selected in an 834 bp-long open reading frame (ORF) whose sequence was retrieved from *L. murinus* IRSD_2020 genome and was found with >99% similarity in other *L. murinus* strains and with <77% similarity in *Streptococcus suis* (**Figure S1**). Primers and probes included in the real-time PCR assay targeting *L. animalis* were selected in the 16S-23S internal transcribed spacer (ITS) region. All the primers and probes (**Table S4**) were designed with TaqMan® Primer and Probes Design Tool (Genescript, Leiden, the Netherlands) and purchased from Eurofins Genomics (Germany). Detection was achieved with LightCycler480II (Roche Diagnostics, Meylan, France) real-time PCR system according to the manufacturer's instructions. TaqMan® qPCRs were performed in 10µL reactions containing: 1X iQ Supermix (Biorad), 0.3µM each primer, 0.2µM probe, 2µl purified DNA diluted 1:10 and nuclease-free water. The bacterial DNA qPCR was performed using the following conditions: 95°C for 3 min, followed by 45 cycles consisting of 95°C for 15 s and 60° for 60 s. Duplicate reactions were run for all samples. The cycle threshold of each sample was then compared with a DNA standard. DNA standard was obtained by purification of *Ligilactobacillus* genomic DNA from the 10ml pellet of overnight culture using the QIAamp Fast DNA Stool Mini Kit (Qiagen, Hilden, Germany). Ten-fold serial dilutions of DNA standard were used to generate a standard curve. The data was expressed as *Ligilactobacillus* copies per ng of isolated DNA.

Bacterial culture

L. murinus IRSD_2020 was grown on Lactobacilli MRS broth (Difco, Fisher scientific SAS, Illkirch, France) – agar plates supplemented with cysteine chloride monohydrate 0.5g.L-1. After 24 hours of incubation at 37°C, 3 colonies were seeded in 30 mL of MRS broth supplemented with cysteine chloride monohydrate 0.5g.L-1 (Merck–Sigma Aldrich, St. Quentin Fallavier, France) and incubated overnight at 37°C. Cultures have been performed with or without GABA (8 mg/mL; Sigma A2129, St. Quentin Fallavier, France) in the medium. All the culture steps have been performed in a hypoxic environment ensured by using a Whitley H35hypoxystation (don Whitley scientific, Bingley, United Kingdom) and all the incubations were done in an anaeropack jar (Fisher scientific SAS, Illkirch, France) with an

anaeroGen sachet (Fisher scientific SAS, Illkirch, France) to ensure an anaerobic environment. Lipopeptides containing GABA were quantified in these bacteria.

Bacterial lipopeptide quantification

To quantify bacterial lipopeptides, mass-spectrometry method has been adapted from the C12AsnGABA quantification method previously described [7] following our previous manuscript on the mass-spectrometry analyses of aminolipids and lipopeptides [8], [9]. For the extraction, 500µL of Tris buffer (pH=9), 1mL of MeOH and 5µL of IS *C16AsnGABA were added to the bacterial pellets or colon samples and crushed with a Fast Prep instrument (MP Biomedicals), using two cycles (6,5m.s-1, 30s). For the human feces, 300 mg of feces were crushed in 500µL of Tris buffer (pH=9) and 1mL of MeOH as described above. In 1/3 of the extract (500 µL), 5µL of IS *C16AsnGABA and 1 mL of Tris/MeOH were added. Ten µL of suspension were withdraw for protein quantification with Biorad assays, then, 6.6mL of water were added to the homogenate. Samples were centrifuged at 1016 x g for 15min (4°C) and the supernatants submitted to SPE using HLB plates (HLB, 30mg, Waters). Plates were conditioned with 750µL ethyl acetate, 750µL MeOH and 750µL H2O:MeOH (90:10; v/v). Samples were loaded at a flow rate of one drop per 2s and SPE plates washed using 1mL H2O:MeOH (90:10; v/v) followed by 1mL heptane. Lipopeptides were eluted using 1mL AcN, 1mL MeOH and 1mL AcOEt. Eluent were carefully removed from the plate, and transferred to a Pyrex tube, dried under nitrogen gas and reconstituted in 10µL MeOH for LC-QqQ (ou LC-LRMS) analysis. Extract was stored at -20°C before LC-MS analysis. High-performance liquid chromatography system was a Shimadzu Mikros LC system, equipped with a thermostated autosampler SIL-30AC, a rack changer II, a Nexera Mikros binary pump, a degasser on-line DGU-20A3R and a LTO-Mikros column oven. The analytical column was a CSH C18 column Waters (1 x 100mm; 2,7µm) and was maintained at 40°C. The mobile phases consisted of water:FA (99.9:0.1; v/v) (A) and acetonitrile:FA (99.9:0.1, v/v) (B). Flow rate was 0.1mL.min-1. The multi-step gradient starts with 30% B at 0 min, 80% B at 13min, 100% B at 13.5min, 100% B at 16 min, and at 16.5 min 30% B until 18min. The chromatography system was coupled online to a triple quadrupole mass spectrometer Shimadzu 8060 equipped with a ESI source in negative mode and was optimized as follow: nebulizer: 2 L.min-1; desolvation line: 250°C; heating-block: 450°C, heating gaz flow: 10L.min-1, and no drying gas was used. Argon gas (purity, >99.9995%) was used for collision-induced dissociation (CID). For each metabolite the

MRM transition (**Table S5**) was optimized on the pure standard to get the best selectivity and the best sensitivity with a qualitative and a quantitative transition and was programmed to monitor a 2min-window (expected chromatographic retention time ± 1min). The dwelltime were optimized for each compound and were set between 15 and 100msec. Peak detection, integration, and quantitative analysis were performed with LabSolution software (Version 5.99 SP2), Shimadzu.

Calcium imaging of sensory neurons

Mouse dorsal root ganglia were dissociated as previously described [10]. After 48h of culture, cells were incubated with HBSS containing 20mM HEPES, 1mM fluo-4 acetoxymethyl (AM) and 20% pluronic F-127 for 30min at 37ºC plus 30min in the dark at RT. The plates were then washed with HBSS and 140µl of HBSS were added to each well. Neurons were pre-treated with C16LeuGABA (0.1, 1, and 10 µM), or vehicle (HBSS/MeOH 0.06%) for 5 min and then were stimulated with either capsaicin or the mix of GPCR agonists. Live cell imaging of calcium was carried out on an automated inverted microscope (Axio Observer, Zeiss, SAS France) with a x10 objective (NA 0.45). Images were acquired using the Zen imaging software (3.1 Blue Edition) and a kinetic of 85 recordings (one per second) was performed. The first ten images were used to determine the baseline and, from 10 to 60 sec, neurons were exposed to either a mix of GPCR agonists (histamine, bradykinin, serotonin, 10 µM), capsaicin (500 nM) or vehicle (HBSS). After 60 seconds, neurons were treated with KCl (50 mM) in order to discriminate neurons from glial cells. The ImageJ software was used to perform the analysis of calcium flux.

Statistical analysis

To perform a multivariate analysis of our cohort, the data obtained from 56 mice (4 groups with 14/group) from 3 different experiments were used to create a matrix including different variables: gene expression, PUFA quantification, VMR to colorectal distension, faecal bacteria abundance from the 16S RNA sequencing, and colon thickness. Principal Component Analysis (PCA) were performed to detect outliers and intrinsic clusters. Then PLS-DA was applied to study the relationship between prenatal stress exposure and variables described above. From this analysis, discriminant variables (with a value of Variance Importance in the Projection, VIP, > 1.0) were selected. Wilcoxon test with FDR correction was applied on

selected variables. PCA, PLS-DA and Wilcoxon test were done using the Galaxy Workflow 4 metabolomics (W4m) instance [11], [12]. Correlations were performed by Spearman test.

Data are presented as means ± standard error of the mean (SEM). Analyses were performed using GraphPad Prism 9.0 software (GraphPad, San Diego, CA). Due to the small sample size and scoring, comparisons between groups were mainly performed by Mann-Whitney non-parametric test. Multiple comparisons within groups were performed by Kruskal-Wallis test, followed by Dunn's post-test. Parametric two-way Anova was used when data were linearly distributed and followed by Bonferroni posthoc test. Statistical significance was set at $P < 0.05$.

Supplementary Table

Supplementary Table S1 PUFA metabolites quantification. Concentration of PUFA metabolites (pg/mg of proteins) in colons of control female (F-CTRL), prenatal stress female (F-PS), control male (M-CTRL) and prenatal stress male (M-PS) mice. Data are expressed as mean ± SEM. Statistical analysis was performed independently for each sex using a Mann-Whitney test. * P<0.05 compared to M-CTRL group.

	Mean ± SEM F-CTRL	**Mean ± SEM F-PS**	**Mean ± SEM M-CTRL**	**Mean ± SEM M-PS**
6kPGF$_{1\alpha}$	84094 ± 11155	96460 ± 18129	102285 ± 15010	83319 ± 10955
TxB2	14186 ± 2248	14363 ± 2054	14363 ± 2249	12422 ± 1552
PGE$_3$	119 ± 809,1	1088 ± 872,1	1043 ± 638,4	1124 ± 55,1
12-TriHOME	7403 ± 3675	6269 ± 4019	10106 ± 5272	9080 ± 7630
PGF$_{2\alpha}$	39315 ± 22747	38106 ± 30182	38567 ± 20861	34640 ± 21751
10-TriHOME	7273 ± 1151	7119 ± 1566	9635 ± 1476	10005 ± 2792
PGE$_2$	81692 ± 13047	81306 ± 14619	73924 ± 10831	67333 ± 9001
PGD$_2$	41575 ± 6777	47094 ± 10117	45921 ± 7468	35403 ± 5002
LxA4	299.6 ± 51.17	284.3 ± 64.08	451.7 ± 68.48	235 ± 41.8*
8isoPGA$_2$	3722 ± 813.1	3405 ± 635.5	2630 ± 553.5	2493 ± 497.6
PDx	63.35 ± 12.37	74.99 ± 16.27	44.32 ± 8.56	36.82 ± 7.55
LTB4	113.4 ± 8.87	128.8 ± 23.45	163.2 ± 46.16	77.65 ± 9.58
12,13-DiHOME	3201 ± 781.4	2712 ± 416.4	2846 ± 324.9	2315 ± 216.5
9,10-DiHOME	602.9 ± 83.68	672.1 ± 113.9	746.7 ± 86.87	576.8 ± 64.65
LTB5	12.32 ± 4.34	8.33 ± 2.95	18.97 ± 4.42	17.52 ± 5.56
9-HOTrE	252.2 ± 52.88	188.4 ± 45.42	339.9 ± 78.27	212.6 ± 48.24
18-HEPE	410.1 ± 75.52	424.5 ± 96.65	649.7 ± 105.2	417.2 ± 86.42
13-HOTrE	241.6 ± 37.01	191.1 ± 36.55	320.3 ± 62.67	305.7 ± 65.08
15-dPGJ$_2$	82.09 ± 18.78	98.98 ± 23.00	70.59 ± 15.24	51.02 ± 8.75
10-HODE	190.3 ± 22.19	223.8 ± 41.89	230.5 ± 22.65	158.4 ± 20.65*
13-HODE	96459 ± 10779	106878 ± 20588	98568 ± 10658	80067 ± 10688
9-HODE	61730 ± 8921	75650 ± 16158	61870 ± 8096	51689 ± 7987
15-HETE	34319 ± 5276	41162 ± 8370	37463 ± 5563	26467 ± 4157

17-HDoHE	11854 ± 1707	13107 ± 3004	9557 ± 1285	7839 ± 1297
13-oxoODE	12419 ± 1454	12511 ± 2367	14612 ± 2094	10072 ± 1406
14-HDoHE	8166 ± 1339	9148 ± 2303	7357 ± 1150	5853 ± 1105
8-HETE	1099 ± 162.9	1349 ± 281.1	1380 ± 222.1	834.9 ± 138.8*
12-HETE	34723 ± 6109	41615 ± 9584	39692 ± 8183	26444 ± 4933
9-oxoODE	12085 ± 1485	11803 ± 1944	13002 ± 1591	9445 ± 905.4
5-HETE	10863 ± 1769	11411 ± 2329	14354 ± 2112	8022 ± 1291*
14,15-EET	61.07 ± 9.75	104.0 ± 16.97	135.0 ± 16.54	71.73 ± 9.02*
5-oxoETE	4592 ± 681.1	5792 ± 1210	8173 ± 1256	4137 ± 717.6*
11,12-EET	147.2 ± 24.94	192.0 ± 44.51	202.0 ± 33.52	94.37 ± 16.43*
8,9-EET	1023 ± 230.2	1078 ± 253.4	1426 ± 254.7	794.2 ± 185.0
5,6-EET	441.4 ± 52.25	542.4 ± 94.27	789.1 ± 95.48	413.3 ± 59.73*

Supplementary Table S2 gene expression quantification. mRNA expression (-Δct) in colons of control female (F-CTRL), prenatal stress female (F-PS), control male (M-CTRL) and prenatal stress male (M-PS) mice. Data are expressed as mean ± SEM. Statistical analysis was performed independently for each sex using a Mann-Whitney test. * P<0.05 compared to M-CTRL group.

	Mean ± SEM F-CTRL	**Mean ± SEM F-PS**	**Mean ± SEM M-CTRL**	**Mean ± SEM M-PS**
Alox15	-4.80 ± 0.23	-5.03 ± 0.24	-5.98 ± 0.41	-5.34 ± 0.27
Alox5	-6.79 ± 0.08	-6.80 ± 0.12	-7.07 ± 0.18	-6.87 ± 0.09*
Ptgs1	-2.65 ± 012	-2.68 ± 0.08	-2.46 ± 0.13	-2.44 ± 0.11
Ptgs2	-4.32 ± 0.11	-4.22 ± 0.25	-4.00 ± 0.21	-4.20 ± 0.20
Alox12	-8.20 ± 0.19	-7.82 ± 0.23	-7.94 ± 0.30	-8.01 ± 0.19
Penk	-4.65 ± 0.13	-4.82 ± 0.13	-4.80 ± 0.29	-4.73 ± 0.11
Ccl5	-6.31 ± 0.23	-6.56 ± 0.15	-6.41 ± 0.22	-6.44 ± 0.15
Ifng	-13.96 ± 0.34	-13.47 ± 0.35	-13.89 ± 0.36	-13.56 ± 0.21
Tgfb	-2.37 ± 0.08	-2.29 ± 0.08	-1.96 ± 0.14	-1.92 ± 0.11
Il6	-8.58 ± 0.68	-8.31 ± 0.78	-7.49 ± 0.73	-7.44 ± 0.72
Il1b	-4.75 ± 0.53	-4.70 ± 0.49	-4.13 ± 0.65	-4.33 ± 0.59
Cxcl2	-5.58 ± 0.71	-5.40 ± 0.70	-4.84 ± 0.82	-5.02 ± 0.78
Tnfa	-6.03 ± 0.17	-5.90 ± 0.16	-5.56 ± 0.18	-5.81 ± 0.15
Tff3	-0.13 ± 1.19	-0.23 ± 1.21	-0.48 ± 1.43	-0.06 ± 1.21
Occludine	-0.58 ± 0.15	-0.50 ± 0.13	-0.46 ± 0.15	-0.47 ± 0.15
Nfkb	-1.25 ± 0.11	-1.07 ± 0.13	-0.94 ± 0.09	-0.86 ± 0.11
Ppara	-5.41 ± 0.25	-5.69 ± 0.28	-5.07 ± 0.25	-5.08 ± 0.20
Tjp1	-0.24 ± 0.15	-0.27 ± 0.11	0.37 ± 0.07	0.26 ± 0.10
Acot12	-11.16 ±0.10	-11.40 ± 0.12	-10.29 ± 0.44	-10.55 ± 0.48
Angptl4	-5,40 ± 0.20	-5,49 ± 0.21	-5.52 ± 0.24	-5.70 ± 0.18
Muc2	3.13 ± 0.12	3.41 ± 0.10	3.57 ± 0.27	3.30 ± 0.16
Mmp7	-5.72 ± 1.21	-5.28 ± 1.28	-4.07 ± 1.58	-5.52 ± 1.31
Cd36	-3.22 ± 0.14	-3.05 ± 0.15	-3.11 ± 0.17	-3.21 ± 0.16
Ahr	-0.68 ± 0.84	-0.85 ± 0.71	-0.13 ± 1.13	-0.86 ± 0.68
Ephx2	-1.69 ± 0.96	-1.86 ± 0.92	-1.20 ± 1.31	-2.05 ± 0.91
Reg3g	-9.35 ± 0.30	-9.37 ± 0.22	-9.22 ± 0.28	-9.35 ± 0.32

Supplementary Table S3 QPCR Primers

Transcript	Forward	Reverse
Hprt	GTTCTTTGCTGACCTGCTGGAT	CCCCGTTGACTGATCATTACAG
Alox15	TCCGGGGATGGAGAAGCTACA	TCCGCTTCAAACAGAGTGCCT
Alox5	TCTTCCTGGCACGACTTTGCTG	GCAGCCATTCAGGAACTGGTAG
Ptgs1	CACTTCTATGCTGGTGGACTATG	CTTGATGACATCCACAGCCACAT
Ptgs2	TCAAGACAGATCATAAGCGAG	AAAGGCGCAGTTTATGTTGTC
Alox12	TGTTGCCACCATGAGATGCCT	CCACCTGTGCTCACTACCTGA
Penk	CGACATCAATTTCCTGGCGT	AGATCCTTGCAGGTCTCCCA
Ccl5	ACTCCCTGCTGCTTTGCCTAC	TTCCTTCGAGTGACAAACACGA
Ifng	CAGCAACAGCAAGGCGAAA	AGCTCATTGAATGCTTGGCG
Tgfb	GACCCCCACTGATACGCCT	GCTGAATCGAAAGCCCTGTA
Il6	TCTGGGAAATCGTGGAAATGAG	TTCTGCAAGTGCATCATCGTTG
Il1b	ACCTTCCAGGATGAGGACATGAG	CATCCCATGAGTCACAGAGGATG
Cxcl2	AGCCCCCCTGGTTCAGAAA	TCCAGGTCAGTTAGCCTTGCC
Tnfa	CCACGCTCTTCTGTCTACTGAAC	GGTCTGGGCCATAGAACTGATG
Tff3	TGCAGATTACGTTGGCCTGTC	TGGAGTCAAAGCAGCAGCC
Ocln	TGGATGACTACAGAGAGGAGAGT	TCCTCTTGATGTGCGATAATTTGC
Nfkb	ATGGCCCATACCTTCAAATAT	TCTCACTAGAGGCTCCCGGAA
Ppara	CCCTGTTTGTGGCTGCTATAATTT	GGGAAGAGGAAGGTGTCATCTG
Tjp1	GTTGGTACGGTGCCCTGAAAGA	GCTGACAGGTAGGACAGACGAT
Acot12	GGTGGTAAATGGAGACAAAC	ACGGCAGCACAACTGACCTTA
Angptl4	CTCCCAACGCCACCCACTTA	GCTGGATCTGGAAAAGTC
Muc2	CGGAACTCCAGAAAGAAGCCA	GGCAGTCAGACGCAAAGTTGTA
Mmp7	ACTGATGGTGAGGACGCAGG	CATCACAGTACCGGGAACAGAA
Cd36	ATGACGTGGCAAAGAACAGC	GAAGGCTCAAAGATGGCTCC
Ahr	CGCTTGATTTACAGAAATGGA	ATCTCGTACAACACAGCCTC
Ephx2	CGTTTATGCCACCAGATCCTGAT	ATGTTCTTCTCCAGTTCAGCCT
Reg3g	CCTCCATGATCAAAAGCAGTGG	GGATTCGTCTCCCAGTTGATGT
Nr3c1	TGGAGAGGACAACCTGACTTCC	ACGGAGGAGAACTCACATCTGG

Supplementary Table S4 Primers and probes used for TaqMan® real-time PCR assays

Target strain	Forward primer, reverse primer and probe sequence (5' - 3') *	Tm (°C)	Amplicon size (bp)
L. animalis DSMZ 20602	CTTTGCACGCAGGAGGTC	56	131
	CGCGGTGTTCTCGGTTATTT	56	
	FAM-ACGGTTCGATCCCGTTAAGCTCCA-TAMRA	62	
L. murinus IRSD_2020	CAAGAGAGTCGCTTACCAGAT	54	120
	ACCGATCTCATCTGCTGGTAG	56	
	FAM-CACCCGAAACAGTTGCAAAGCCTCT-TAMRA	62	

* FAM, 6-*carboxyfluorescein; TAMRA, tetramethylrhodamine*

Supplementary Table S5 SRM characterization with quantitative and qualitative transition, energy applied to generate the transition (EC et Q1/Q3PreBias), and retention time.

Compound	Quantitative MRM transition	Q1 Pre Bias (V)	EC (eV)	Q3 Pre Bias (V)	Qualitative transition	Retention time (min)
C12AlaGABA	384 → 366	30	11	18	384 → 102	6.3
C14AsnGABA	426 → 102	21	13	17	426 → 114	7.56
C14:1AlaGABA	381 → 102	27	31	25	381 → 88	7.82
C12ValGABA	383 → 280	12	31	27	383 → 102	8.28
C12LeuGABA	397 → 130	19	31	18	397 → 102	9.00
C14GABA	312 → 226	24	21	12	312 → 102	9.96
C14IleGABA	425 →130	22	31	20	425 → 102	11.23
C16LeuGABA	453 →130	18	34	17	453 → 130	13.53
C16PheGABA	487 → 384	19	27	19	487 → 102	13.72
C16GluGABA	465 → 102	23	37	10	465 → 96	9.13

Supplementary figures

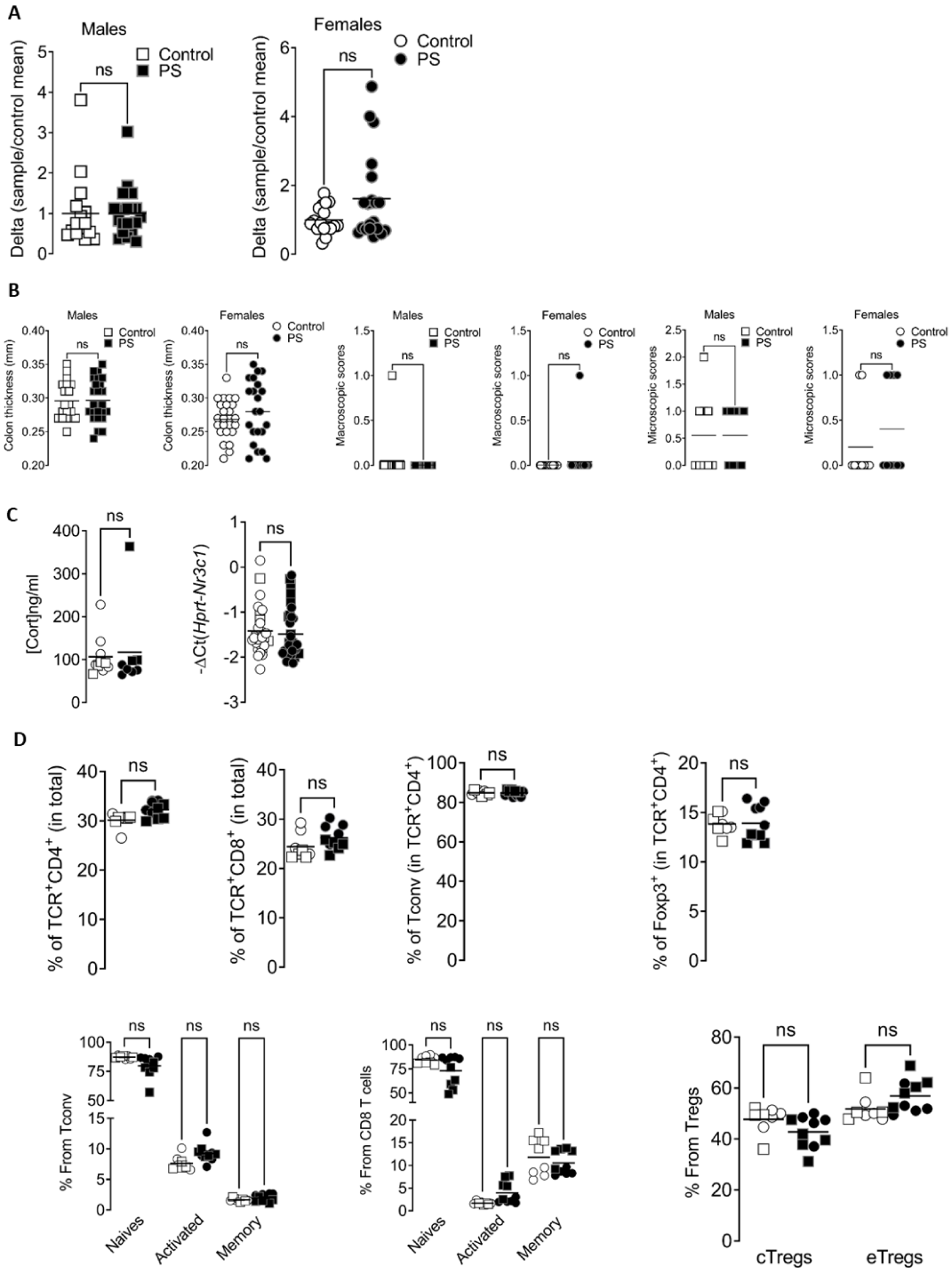

Figure S1:

(A) Intestinal paracellular permeability was monitored 4 hours after oral administration of FITC dextran 4 kDa. FITC fluorescence was quantified in the serum of control mice (white) or

PS mice (black), in the male (square) and female (circle) offspring. Data are expressed as scatter dot plot with the mean. Statistical analysis was perform using a Mann-Whitney test. (n=12-22 mice/group, 3 independent experiments). **(B)** Colon thickness, macroscopic and microscopic colon damage scores of control mice (white) or PS mice (black), in the male (square) and female (circle) offspring. Data are expressed as scatter dot plot with the mean (ctrl male vs PS male and Ctrl female vs PS female; n= 10-24 mice/group, 3 independent experiments). **(C)** Plasmatic corticosterone concentration and its receptor expression in the colon were determined in control mice (white) or prenatal stress (PS) mice (black), in the male (square) and female (circle) offspring. Data are expressed as scatter dot plot with the mean. ns: not significant. **(D)** 14 weeks old males (square) and females (circle) controls (while symbols, n=8) or prenatally stressed (black symbols, n=10) were euthanized and their mesenteric lymph node cells were analyzed by flow cytometry. The upper panel represent the proportion of the different major T cell populations in individual mice. The lower panel represent the activation status of T cell populations based on their expression of CD62L and CD44. Data are expressed as scatter dot plot with the mean. ns: not significant.

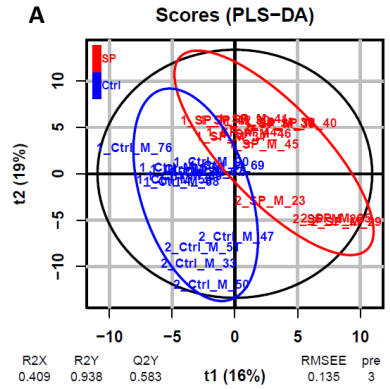

B

Variable	FDR
Colorectal distension total AUC	0.029
14,15-EET	0.033
11,12-EET	0.046
5,6-EET	0.046
L.murinus/animalis	0.046
Erysipelotrichia unknown	0.046
Desulfovibrio sp	0.046
Bacteria unclassified	0.0033

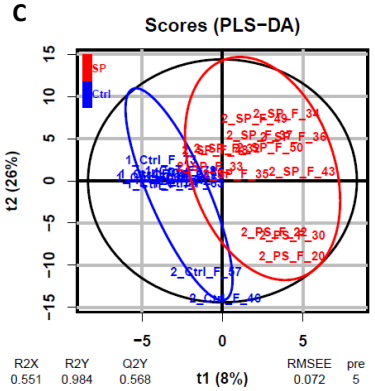

D

Variable	FDR
Colorectal distension total AUC	0.012
Clostridiales unknown	0.012
Akkermansia muciniphila	0.0042

Figure S2. PS and Ctrl mice separation in PLS-DA can be explained by visceral pain sensitivity and different bacterial abundances in male and female. Multivariate analysis of the male cohort **(A, B)** and female cohort **(C, D)**: **(A-C)** Two-dimensional PLS-DA score plots for **(A)** males ((R2X = 40.9%, R2Y = 93.8%, Q2=0.583), 28 samples (control, n = 14, blue; PS, n = 14, red)) and **(C)** females ((R2X = 55.1%, R2Y = 98,4%, Q2=0.568), 25 samples (control, n = 12, blue; PS, n = 13, red)). Each dot corresponds to an individual. The black ellipse corresponds to a 95% confident interval based on the Hotelling's T^2. **(B-D)** Discriminant (Variable Importance in Projection > 1) and significant (FDR-corrected p value of Wilcoxon test < 0.05) variables for male **(B)** and female **(D)**.

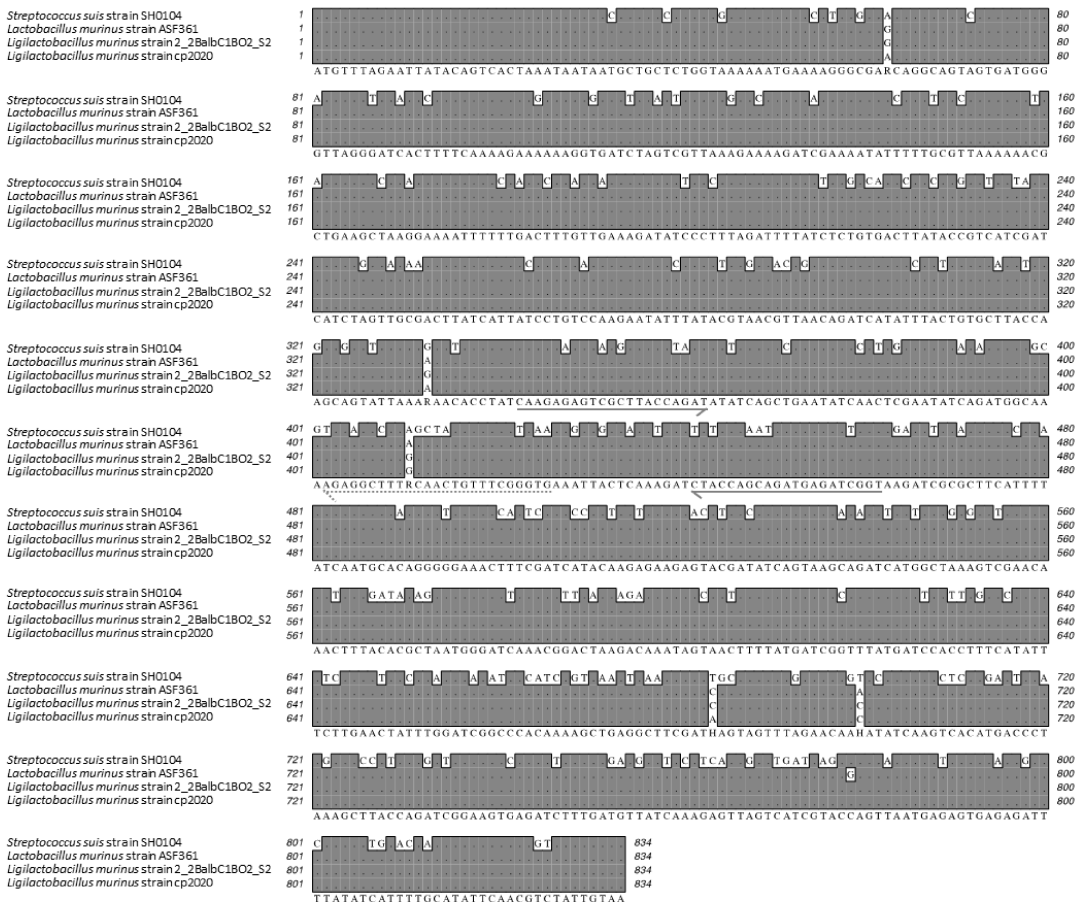

Figure S3. Primers and probe designed for the *L. murinus* specific real-time PCR assay. The nucleotide sequence of an open reading frame (ORF) identified in the *L. murinus* strain IRSD_2020 was aligned with those of a nearly identical ORF found in *L. murinus* strains ASF361 and 2_2BalbC1BO2_S2, and an ORF with less than 77% similarity found in *Streptococcus suis* strain SH0104. Identical and different nucleotides are reported with grey and white background, respectively. Solid and dashed arrows (5' to 3' orientation) indicate the positions of the primers and probe, respectively, which were selected in locations displaying nucleotide variability, in order to specifically target *L. murinus* IRSD_2020 by real-time PCR.

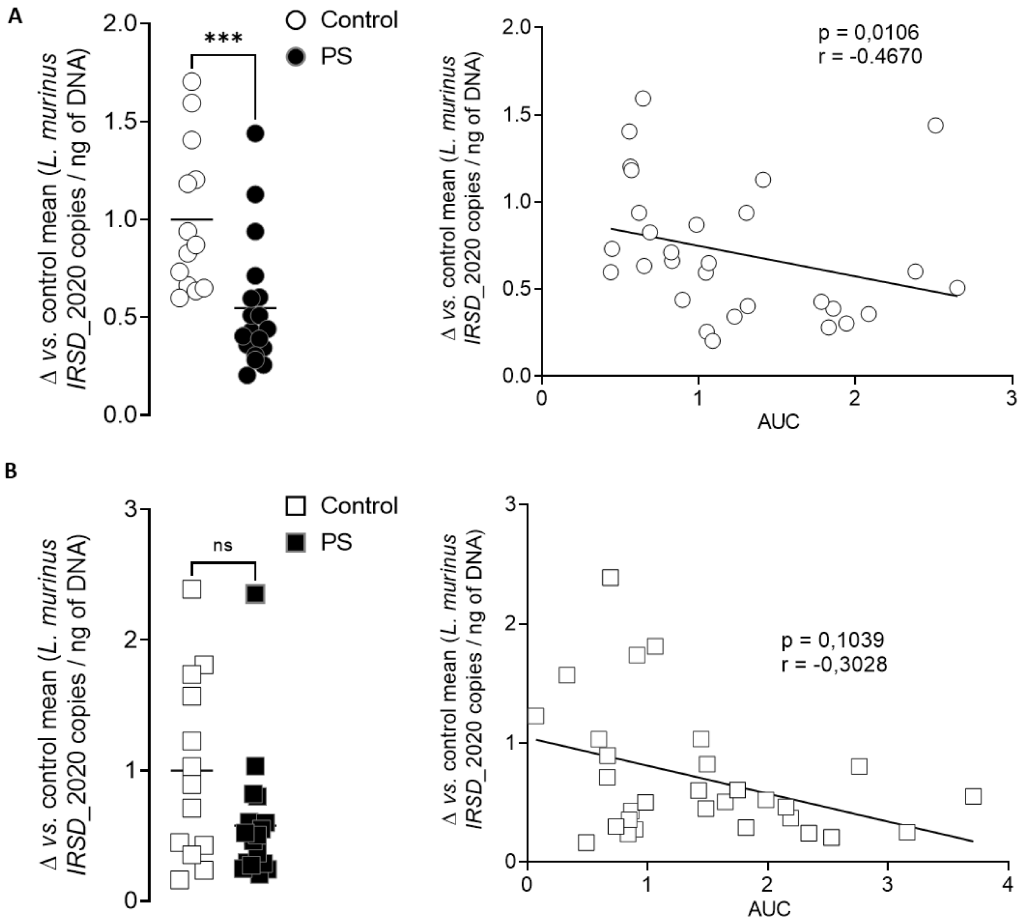

Figure S4: *L. murinus* IRSD_2020 concentration is decreased in PS female mouse feces

The levels of the *L. murinus* strain IRSD_2020 were quantified by TaqMan® real-time PCR in the feces of control mice (white) or PS mice (black), in the female (**A**, circle) and male (**B**, square) offspring. Data are expressed as scatter dot plot with the mean. Statistical analysis was performed using a Mann-Whitney test. ***p<0.001, significantly different from the control group (n=13-18 male mice/group and n=14-18 female mice/group, 3 independent experiments). Spearman correlations were used to analyze the correlation between the fecal bacteria quantity and visceral motor response to colorectal distension expressed in AUC, in male (square) and female (circle) offspring. P and r values are indicated on each graph.

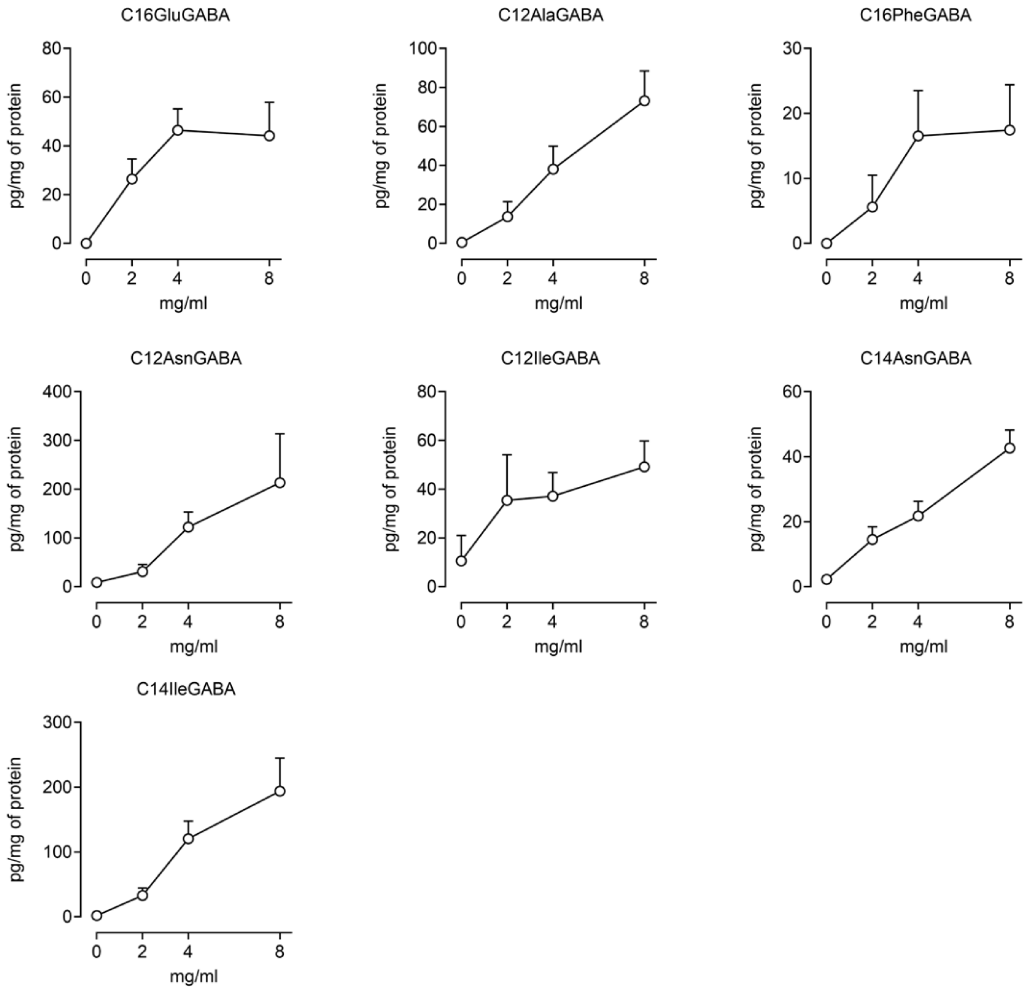

Figure S5*. L. murinus* IRSD_2020 produces GABA-lipopeptides. Concentration of lipopeptides quantified by LC-MS/MS in the bacterial pellets of *L. murinus* IRSD_2020 cultivated without (0 mg/mL) or with GABA (2, 4 or 8 mg/mL). Data are expressed as scatter dot plot with the mean (n=9).

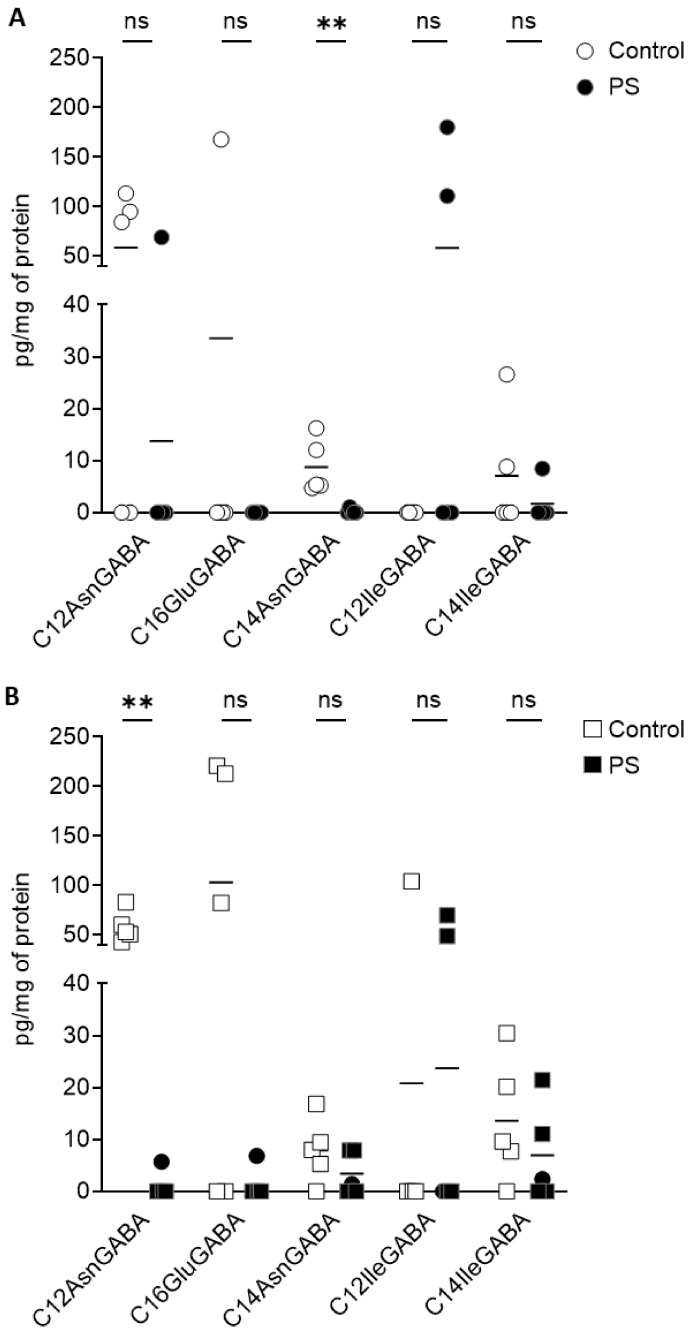

Figure S6: Concentration of C12AsnGABA and of C14AsnGABA is decreased in PS female and PS male mouse, respectively. (B) Individual (left panel) and total (right panel) concentration of lipopeptides quantified by LC-MS/MS in the colon of female (**A**, circle) and male (**B**, square) control (white) and PS mice (black). Data are expressed as scatter dot plot with the mean (n=5 female mice and n=4-5 male mice). Statistical analysis was performed using a Mann-Whitney test. *p<0.05, **p<0.01, significantly different from the corresponding control group

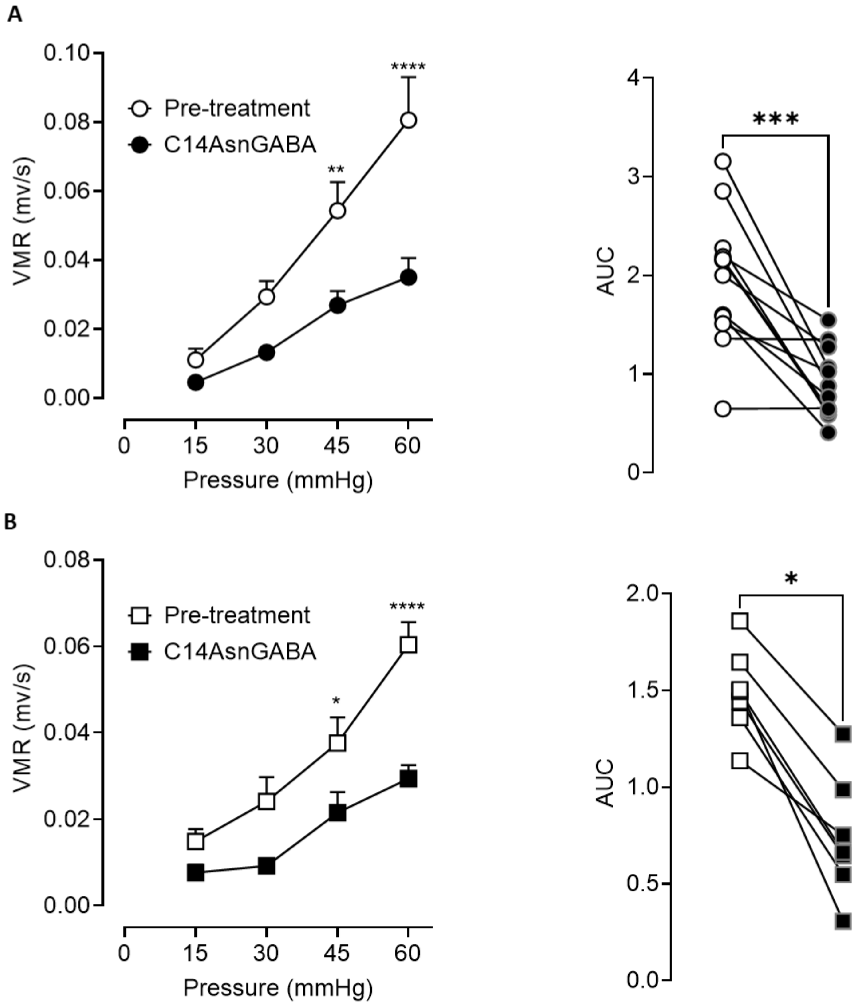

Figure S7: C14AsnGABA administration decrease PS-induced visceral hypersensitivity in male and female mice. Visceral motor response to colorectal distensions (VMR) in response to increasing pressures of distension (15, 30, 45 and 60 mmHg) was measured, in both female (**A**) and male (**B**) PS offspring. Measurements were done before (white) and after intracolonic administrations of C14AsnGABA (black). Data are expressed as mean ± SEM (n=12 female mice/group and n=7 male mice/group, 2 independent experiments mixing male and female). Statistical analysis was performed using two-way Anova analysis of variance and subsequent Sidak's multiple comparison test. *P<0.05, **p<0.01, ****p<0.0001 significantly different from pretreatment group. The results are also expressed as area under the curve (AUC) presented as scatter dot plot with the mean. Statistical analysis was perform using a Wilcoxon test. *P<0.05, ***p<0.001, significantly different from the pretreatment group.

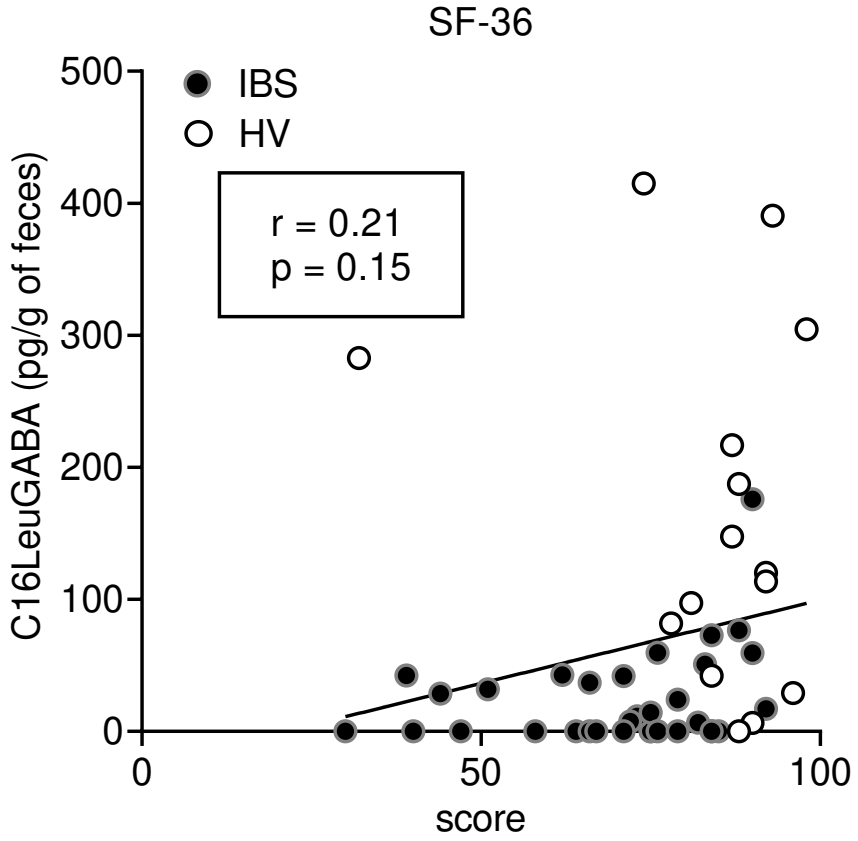

Figure S8. Correlation between C16LeuGABA in feces and SF-36 score. Spearman correlation was used to analyse the correlation between the concentration of CL16LeuGABA and SF-36 score in healthy volunteers (HV, white) and patients with IBS (black). p and r values are indicated on the graph

Supplementary references

[1] J. Boué *et al.*, « Endogenous regulation of visceral pain via production of opioids by colitogenic CD4(+) T cells in mice », *Gastroenterology*, vol. 146, nº 1, p. 166-175, janv. 2014, doi: 10.1053/j.gastro.2013.09.020.

[2] P. Le Faouder *et al.*, « LC-MS/MS method for rapid and concomitant quantification of pro-inflammatory and pro-resolving polyunsaturated fatty acid metabolites », *J. Chromatogr. B Analyt. Technol. Biomed. Life. Sci.*, vol. 932, p. 123-133, août 2013, doi: 10.1016/j.jchromb.2013.06.014.

[3] S. Nicolas *et al.*, « Transfer of dysbiotic gut microbiota has beneficial effects on host liver metabolism », *Mol. Syst. Biol.*, vol. 13, nº 3, p. 921, mars 2017, doi: 10.15252/msb.20167356.

[4] N. Segata *et al.*, « Metagenomic biomarker discovery and explanation », *Genome Biol.*, vol. 12, nº 6, p. R60, juin 2011, doi: 10.1186/gb-2011-12-6-r60.

[5] M. G. I. Langille *et al.*, « Predictive functional profiling of microbial communities using 16S rRNA marker gene sequences », *Nat. Biotechnol.*, vol. 31, nº 9, p. 814-821, sept. 2013, doi: 10.1038/nbt.2676.

[6] O. Hammer, D. A. T. Harper, et P. D. Ryan, « PAST: Paleontological Statistics Software Package for Education and Data Analysis », p. 9.

[7] T. Pérez-Berezo *et al.*, « Identification of an analgesic lipopeptide produced by the probiotic Escherichia coli strain Nissle », *Nat. Commun.*, vol. 8, nº 1, déc. 2017, doi: 10.1038/s41467-017-01403-9.

[8] A. Hueber *et al.*, « Identification of bacterial lipo-amino acids: origin of regenerated fatty acid carboxylate from dissociation of lipo-glutamate anion », *Amino Acids*, vol. 54, nº 2, p. 241-250, févr. 2022, doi: 10.1007/s00726-021-03109-1.

[9] A. Hueber *et al.*, « Discovery and quantification of lipoamino acids in bacteria », *Anal. Chim. Acta*, vol. 1193, p. 339316, févr. 2022, doi: 10.1016/j.aca.2021.339316.

[10] N. Cenac *et al.*, « Potentiation of TRPV4 signalling by histamine and serotonin: an important mechanism for visceral hypersensitivity », *Gut*, vol. 59, nº 4, p. 481-488, 2010, doi: 10.1136/gut.2009.192567.

[11] E. A. Thévenot, A. Roux, Y. Xu, E. Ezan, et C. Junot, « Analysis of the Human Adult Urinary Metabolome Variations with Age, Body Mass Index, and Gender by Implementing a Comprehensive Workflow for Univariate and OPLS Statistical Analyses », *J. Proteome Res.*, vol. 14, nº 8, p. 3322-3335, août 2015, doi: 10.1021/acs.jproteome.5b00354.

[12] Y. Guitton *et al.*, « Create, run, share, publish, and reference your LC-MS, FIA-MS, GC-MS, and NMR data analysis workflows with the Workflow4Metabolomics 3.0 Galaxy online infrastructure for metabolomics », *Int. J. Biochem. Cell Biol.*, vol. 93, p. 89-101, déc. 2017, doi: 10.1016/j.biocel.2017.07.002.